

# Recent advances in functional supramolecular nanostructures assembled from bioactive building blocks

Yong-beom Lim, Kyung-Soo Moon and Myongsoo Lee\*

Received 28th August 2008

First published as an Advance Article on the web 20th January 2009

DOI: 10.1039/b809741k

Supramolecular nanostructures covered with bioactive functional molecules have been actively explored as promising materials in the field of biotechnology. Recent advances in nano-sized chemistry have made it possible to fabricate various kinds of nanostructures with tailor-made nanostructural properties. This, combined with appropriate bioactive functionalization, has led to the successful utilization of supramolecular nanostructures in diverse biomaterials applications. This *tutorial review* describes the concept, current developments, and prospects of self-assembled bioactive nanostructures, which are assembled directly from bioactive supramolecular building blocks.

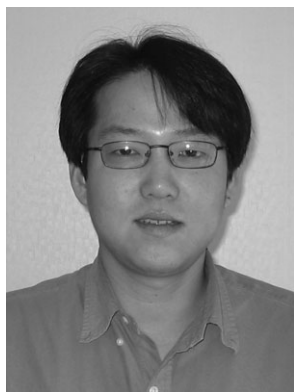
## 1. Introduction

Research on nanometre-sized structures has become one of the fastest growing fields of science. The application potential of nanostructures is diverse, ranging from electronic and detection materials to biomaterials. The most important reason for their popularity is that they are small. From the standpoint of a biological system, submicron-sized nano-objects are generally much smaller than most cells, but are similar in size to many subcellular components (proteins and DNA), cellular organelles (mitochondria, lysosomes, ribosomes, and cytoskeleton), and microorganisms (viruses). Most eukaryotic cells have a typical size of a few tens of microns in diameter. Then the submicron-sized biological objects can be regarded as 'biological nanostructures' as compared to 'synthetic nanostructures'.

Self-assembly can be defined as the spontaneous organization of disordered molecular units into ordered structures as a consequence of specific, local interactions among the components themselves.<sup>1</sup> Molecular self-assembly is referred to as a 'bottom-up' approach in contrast to a 'top-down' technique where the desired final structure is carved from a larger block of matter. In fact, the formation of most biological nanostructures is also driven by the self-assembly process. Examples include the self-assembly of phospholipids to form cell membranes, the formation of a DNA double helix through specific hydrogen bonding of individual strands, and the folding of a polypeptide chain to form protein tertiary or quaternary structure. As we can find nice examples of self-assembled nanostructures in biological systems, it is not surprising that many synthetic nanostructures have been constructed with inspiration from Nature.

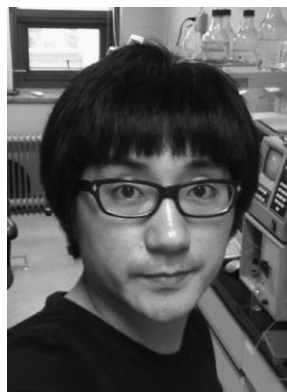
The subject of this tutorial review is bioactive synthetic nanostructures (Fig. 1). We will focus mainly on the nanostructures assembled from functional supramolecular building blocks where the bioactive function and the self-assembling

Center for Supramolecular Nano-Assembly, Department of Chemistry, Yonsei University, Shinchon 134, Seoul 120-749, Korea.  
E-mail: mslee@yonsei.ac.kr; Fax: +82 2 393 6096;  
Tel: +82 2 2123 2647



Yong-beom Lim

Yong-beom Lim received his BS degree in chemistry from Sungkyunkwan University, and MS and PhD degrees in chemistry/biochemistry from Seoul National University, Korea. He did his postdoctoral research at the Department of Biochemistry & Biophysics, University of California, San Francisco (UCSF) until 2006. He is currently a research professor at the Center for Supramolecular Nano-Assembly and Department of Chemistry at Yonsei University. His current research interests are focused on bioactive supramolecular nanostructures.



Kyung-Soo Moon

Kyung-Soo Moon received his BS and his MS degree in Chemistry from Yonsei University and is now a graduate student pursuing his PhD degree at Yonsei University under the supervision of Prof. Myongsoo Lee. His current research interests are functional supramolecular structures and self-assembly of bioactive peptide building blocks.

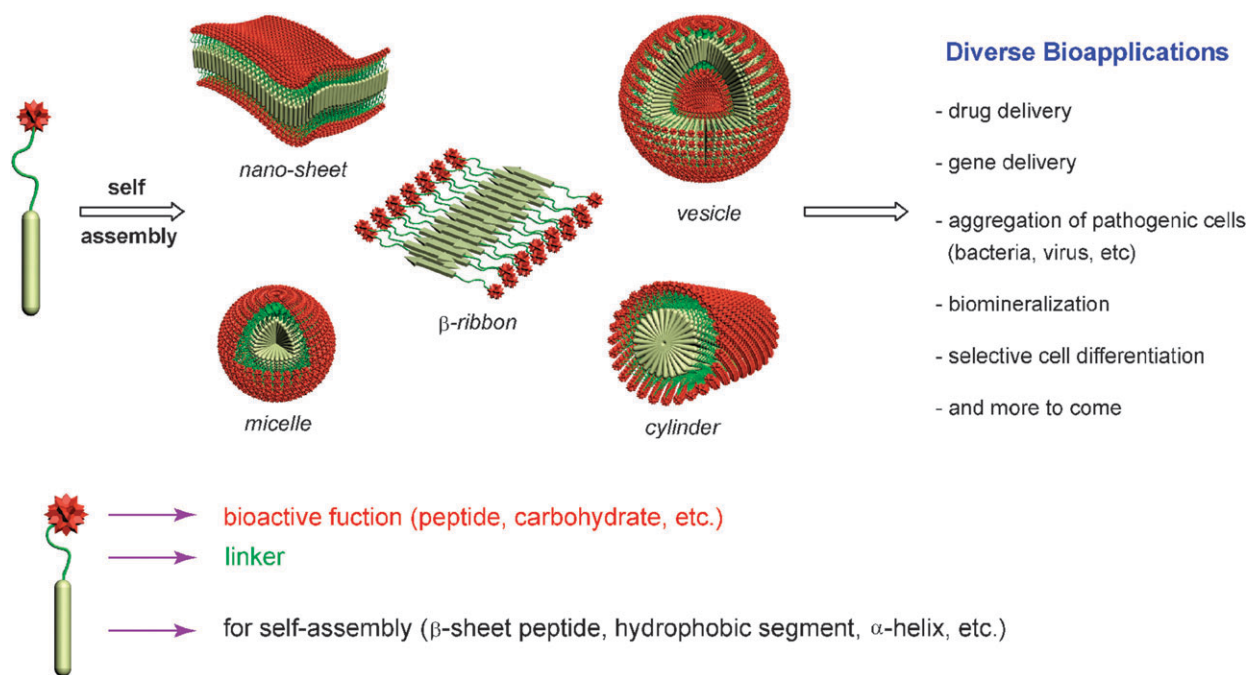


**Fig. 1** Self-assembled bioactive nanostructures.

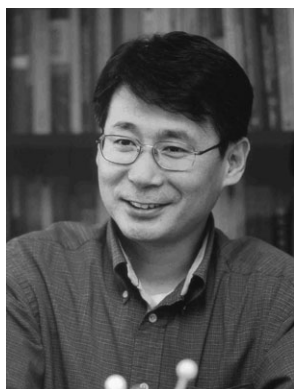
segment are conjugated together. Emphasis will also be placed on the self-assembled nanostructures from synthetic building blocks whose molecular weight distributions are monodisperse. In general, such monodisperse (*i.e.*, homogeneous) building blocks have the advantage of displaying highly reproducible, predictable, and dynamic self-assembly behavior. In addition, the molecular weight of the monodisperse building blocks is relatively smaller than that of most polymeric self-assembly systems. In fact, the scope of bioactive nanostructures can be broad. In addition to the monodisperse system described above, traditional polymer assemblies (polydisperse system), bioactive nanoparticles (non-supramolecular system), DNA assemblies (usually a complexation-based system), and virus assemblies (building blocks of biological

origin) can also be considered as bioactive nanostructures. Interested readers are advised to consult related reviews and research papers on the subjects.<sup>2–10</sup>

#### Molecular self-assembly in aqueous solution

Water is the ubiquitous and indispensable solvent for the existence of a biological system. For that reason, nearly all of the biological self-assembly processes take place in an aqueous environment. For the self-assembly of natural or synthetic molecules in aqueous solution, the molecules interact with one another *via* many types of non-covalent interactions such as hydrophobic, ionic,  $\pi$ -stacking, and hydrogen bonding interactions.<sup>11–14</sup> Such interactions act sometimes alone or in concert to precisely construct the self-assembled nanostructures.

There are numerous examples of self-assembly processes in biological systems; some of them are quite simple while others are extremely complex. Perhaps one of the most simple and widely known self-assembled structures in a biological system is the lipid membrane structure. The primary force responsible for the formation of the membrane structure is the simple and iterative hydrophobic interactions among amphiphilic lipid molecules. The membrane is composed of two layers of lipids arranged so that their hydrocarbon tails face one another to form a hydrophobic core, while their hydrophilic head groups face the aqueous solutions on either side of the membrane. An example of a very complex biological self-assembly process can be found in protein folding.<sup>15</sup> Protein folding is the physical process by which a polypeptide chain folds into its three-dimensional (3D) global energy minimum conformation. As a variety of interaction and structural parameters are interconnected in the protein folding process, the precise mechanism is still not completely understood. The difference between the self-assembly of membrane and protein is that



**Myongsoo Lee**

*Myongsoo Lee received his BS degree in chemistry from Chungnam National University, Korea and his PhD degree in Macromolecular Science from Case Western Reserve University, Cleveland, in 1992. In the same year he became a post-doctoral fellow at the University of Illinois, Urbana-Champaign. In 1994 he joined the Faculty of Chemistry at Yonsei University, Korea, where he is presently Professor of Chemistry. He is a director of the Center for Supramolecular Nano-Assembly*

*and a member of the editorial board of Chemistry—An Asian Journal. His current research interests include synthetic self-organizing molecules, controlled supramolecular architectures, and organic nanostructures with biological functions.*

many molecules are involved in the membrane formation, in contrast to a single molecule in the protein folding. Similarly to the biological nanostructures, synthetic nanostructures can be constructed by the iterative interactions among supramolecular building blocks, by folding of single polymeric molecules (e.g., foldamers), or by a combination of both.

### Bioactive functionalization: multivalent effect

One of the most important characteristics of nanostructures fabricated by a bottom-up self-assembly process is the multivalent display of desired functional molecules on the surface of nanostructures. The multivalent effect might best be utilized in multivalent interactions.<sup>16–18</sup> Multivalent interactions have unique collective properties that are quite different from properties displayed by monovalent interactions. Multivalent interactions can provide a significant increase in binding affinity that is not achievable with monovalent interactions. In fact, multivalent interactions occur throughout a biological system. These interactions are used as a means to increase binding affinity and specificity of interactions occurring between weakly interacting binding partners.

A traditionally considered multivalent scaffold is a molecule with high-valency reactive functional groups to which all the ligands can be linked covalently (a unimolecular system). Molecules of low valency, generally from di- to octavalent, have been constructed from 1D linear chains or 2D round molecules such as macrocycles. For generating molecules of high valency, polymer or dendrimer scaffolds have been used.

There are advantages and disadvantages of the unimolecular *versus* the self-assembled system. The advantages of the self-assembled multivalent system that can be considered are as follows. First, it is an energy and cost-effective way; instead of making one big multivalent molecule, which often requires multiple synthetic steps, all one needs to synthesize is a simpler monovalent building block and let them aggregate spontaneously. Second, using a self-assembly process is better, especially when it comes to making an object of extremely high valency. Synthesis of polymers or dendrimers, for example, containing more than several thousands of ligands is not practically easy. Moreover, high molecular weight polymers are generally insoluble. Third, there is a rigidity difference.<sup>11,19,20</sup> The conformation of most polymer chains is globular rather than extended, which might act disadvantageously for multivalent interaction with an extended surface area. Self-assembled nanostructures can generally be more rigid than polymeric chains, which can minimize Brownian motion and unfavorable entropic cost associated with ligand–receptor binding events.

## 2. Peptides/proteins as bioactive functional groups

### 2.1 Mode of self-assembly: $\beta$ -sheet interactions

Nanostructures from natural and artificial  $\beta$ -sheet peptides are gaining growing attention as biomaterials, in part due to the fact that they are composed of biocompatible amino acids.<sup>21,22</sup> The  $\beta$ -sheet structure, along with the  $\alpha$ -helix, is one of the main secondary structural elements in proteins. The polypeptide chains are nearly fully extended in a  $\beta$ -sheet structure.

The adjacent  $\beta$ -strands can lie in either a parallel or an antiparallel fashion. In both parallel and antiparallel  $\beta$ -sheets, the  $\beta$ -strands have conformations pointing alternate amino acid side chains to opposite sides of the sheet. Contributions from electrostatic and hydrophobic forces between amino acid side chains on the same face of the sheet often help to stabilize the sheets.

Nanofibers of  $\beta$ -sheet are organized in such a way that each  $\beta$ -strand runs perpendicular to the fibril axis, which is called ‘cross- $\beta$  structure’ (Fig. 2). When one face of the 1D  $\beta$ -sheet structure ( $\beta$ -tape) consists predominantly of hydrophobic side chains, the removal of the hydrophobic chains from contact with water drives two  $\beta$ -tapes to associate into a bilayered  $\beta$ -ribbon structure.

The design principle for most of the artificial  $\beta$ -sheet peptides is the alternating placement of charged (or polar) and hydrophobic amino acids. This type of placement promotes the proper  $\beta$ -sheet hydrogen bonding arrangement between amide hydrogen and carbonyl oxygen. It has been demonstrated that many peptides having a propensity for  $\beta$ -sheet nanofiber formation often laterally interact to form higher order aggregates.<sup>23</sup> Coupling of hydrophilic macromolecules on the N- or C-terminus of  $\beta$ -sheet peptides can significantly inhibit the formation of such higher order aggregates.<sup>24</sup>

Based on these facts, it can be envisioned that coupling of a hydrophilic and bioactive peptide to a  $\beta$ -sheet forming peptide would enable the construction of a discrete 1D nanostructure decorated with bioactive peptides. Substantiation of this idea has recently been reported (Fig. 3).<sup>25</sup> The supramolecular building block, T $\beta$ P, was a block peptide consisting of a cell-penetrating peptide (CPP) Tat<sup>26</sup> (a hydrophilic segment) and a  $\beta$ -sheet forming peptide (a self-assembling segment). It was found that the block peptide formed a  $\beta$ -ribbon structure in which  $\beta$ -sheet interaction was the main driving force for the self-assembly. The self-assembly process was more efficient in phosphate-buffered saline (PBS) solution than in pure water, suggesting usefulness of the peptide nanostructure in biological applications. PBS is a buffer of physiological pH and salt concentration. The T $\beta$ P  $\beta$ -ribbons, similarly to conventional amphiphilic block copolymer micelles, were able

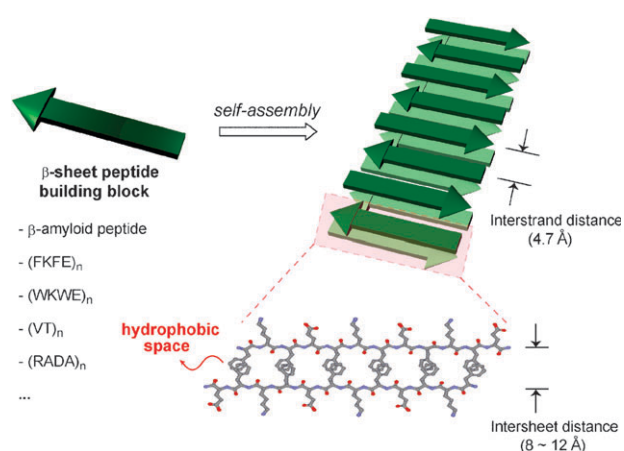


**Fig. 2** Self-assembly of  $\beta$ -sheet peptides into a bilayered  $\beta$ -ribbon structure.

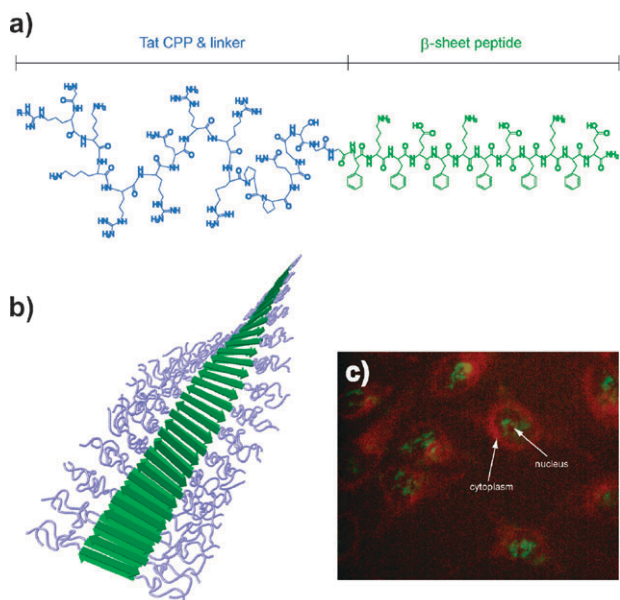


**Fig. 3** (a) Structure of TBP peptide building block. (b) Structure of Tat CPP-coated  $\beta$ -ribbon. (c) Intracellular delivery of encapsulated guest molecules by the CPP-coated  $\beta$ -ribbon. In this confocal laser scanning microscope (CLSM) image of HeLa cells, TBP and encapsulated guest molecules are shown in green and red, respectively. Reproduced in part from ref. 25. © 2007 Wiley-VCH Verlag GmbH & Co. KGaA. Used with permission.

to encapsulate hydrophobic guest molecules such as pyrene or Nile red in the hydrophobic space between two  $\beta$ -tapes (see Fig. 2), showing the possibility of use in drug delivery applications. It turned out that the cell penetration efficiency of the TBP  $\beta$ -ribbon was much higher than that of unimolecular Tat-CPP, suggesting that the multivalent coating of CPPs is advantageous in increasing cellular uptake efficiency. This work showed the possibility that peptides composed only of natural amino acids can be developed as functional nanobiomaterials.

Although the advantage of CPPs is their efficient cell internalization, they lack cell specificity. Therefore, the question of whether  $\beta$ -ribbons can be functionalized to become specific to certain cell types, such as cancer cells, can be raised. As an example of specific cell delivery, the RGD-integrin system was explored. The  $\alpha_v\beta_3$  integrin receptor is expressed only on proliferating endothelial cells such as those present in growing tumors.<sup>27</sup> The  $\alpha_v\beta_3$  integrin receptor is one of the most specific markers of tumor vasculature and is an attractive candidate in cancer-targeting strategies. It has been shown that small peptides containing the Arg-Gly-Asp (RGD) amino acid sequence specifically bind to  $\alpha_v\beta_3$  integrin receptor.

A small peptide such as RGD generally possesses a very high conformational flexibility; cyclization of RGD has been shown to be effective in limiting the conformational flexibility, consequently lowering the unfavorable entropy loss upon binding. For this reason, a  $\beta$ -sheet peptide-based building block was synthesized to contain a cyclic RGD motif as a hydrophilic segment (cRGD-FKE).<sup>28</sup> An intracellular delivery experiment revealed that cRGD-FKE  $\beta$ -ribbon can specifically deliver encapsulated guest molecules to cancer cells. This

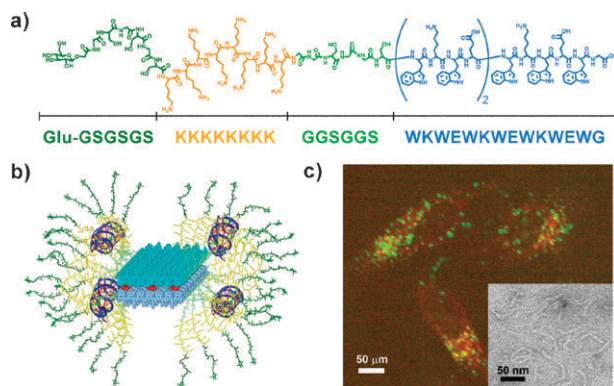


**Fig. 4** (a) Structure of Glu-KW, a building block for the artificial virus formation. A  $\beta$ -sheet peptide segment, nonionic segments (linkers and D-glucose), and a cationic segment are shown in blue, green, and yellow, respectively. (b) Molecular model of the artificial virus incorporating small interfering RNAs (siRNAs; blue, double-helix shape) and hydrophobic guest molecules (red). (c) Intracellular delivery of the artificial virus (green). Inset: TEM image of the artificial virus. Reproduced in part from ref. 29. © 2008 Wiley-VCH Verlag GmbH & Co. KGaA. Used with permission.

result suggests that peptide  $\beta$ -ribbons can be functionalized to become a selective intracellular carrier.

Recently, the creation of a filament-shaped artificial virus by using a  $\beta$ -ribbon as a scaffold was reported (Fig. 4).<sup>29</sup> The building block (Glu-KW) structure is characterized by a  $\beta$ -sheet-forming self-assembly segment, two linker segments, a nucleic acid-binding cationic segment, and a carbohydrate ligand segment. The artificial virus was developed to overcome the problem of current gene carriers, the formation of uncontrollable nanoaggregates. As the nucleic acid-binding cationic segment is shielded by the electrically neutral coats, the artificial virus could retain its original filamentous shape after the gene (siRNA) binding. The artificial virus was highly efficient in simultaneously delivering both siRNA and encapsulated hydrophobic guest molecules, which was attributed to its controlled shape, minimal interaction with serum proteins by the charge-neutral surface, and enhancement of the cell interaction by multivalent coating of carbohydrate ligands. This study provides a general means to control the shape and size of artificial viruses.

Even large proteins could be displayed on the  $\beta$ -ribbons. Barker and co-workers reported the construction of a protein-conjugated building block, in which the  $\beta$ -sheet forming SH3 domain was fused with cytochrome (Cyt), a porphyrin binding protein that catalyzes redox reaction in the cell.<sup>30</sup> The overall size of the building block was 32 kDa, comprising 294 amino acids. The building block was expressed in *E. coli*. Investigations showed that the building block self-assembled into  $\beta$ -ribbon structure as evidenced by a meridional reflection (interstrand distance) at 4.7 Å and an equatorial reflection (intersheet distance) at 9.6 Å in an X-ray fiber diffraction study. Importantly, spectroscopic analyses confirmed that the activity of Cyt was not impaired by the fibril formation, showing that very high densities of proteins can be displayed on the surface of a  $\beta$ -ribbon structure formed from a rationally designed, self-assembling polypeptide fusion protein building block.

In related studies, a  $\beta$ -sheet-forming domain was fused with several different proteins, such as barnase, carbonic anhydrase, glutathione S-transferase, and green fluorescent protein.<sup>31</sup> All fusion proteins formed filamentous nanostructures, whose diameters increased with the mass of the appended enzyme. Remarkably, the activity of the appended enzymes was at most mildly reduced, when substrate diffusion effects were taken into account, indicating that the enzymes retained their native structures even after the fiber formation.

In contrast to the above described direct peptide/protein conjugation methods, indirect methods have also been devised. In one attempt, a 16-amino acid residue  $\beta$ -sheet peptide ( $\beta$ 16) was co-assembled with a biotinylated  $\beta$ 16.<sup>32</sup> Streptavidin modified with colloidal gold was added to the mature nanofibers. TEM investigation revealed that the gold nanoparticles were attached to the nanofibers at regular intervals due to the molecular co-assembly. This study implies that a variety of functional molecules can be noncovalently immobilized on peptide nanofibers in controlled distance and amount.

## 2.2 Mode of self-assembly: hydrophobic interactions

Amphiphilic block molecules, where one of the blocks is hydrophilic and the other hydrophobic, tend to aggregate in selective solvents (good solvent for one block and poor solvent for the other) due to microphase separation between the incompatible blocks. In aqueous solution, the hydrophobic blocks in the amphiphiles tend to associate to form the inner part of the aggregates, while the hydrophilic blocks face the water-exposed outer part. Typically, this type of aggregation behavior has been explored in amphiphilic block copolymers, surfactants, and rod-coil molecules. It has been shown that the amphiphiles can adopt various morphologies depending on the molecular structure, relative volume fraction between hydrophilic and hydrophobic segments, chirality, hydrogen bonding capability, and solvent.<sup>11–14</sup>

Considering the fact that many bioactive peptides are hydrophilic, such a peptide might aggregate to form self-assembled nanostructures if an appropriate hydrophobic segment is attached to the peptide. In fact, such self-assembling peptide–hydrophobe conjugates exist in Nature. In one example, some marine bacteria contain siderophores, iron chelating compounds, which contain a unique peptide head group that coordinates iron and hydrophobic fatty acid tails.<sup>33</sup> Such a possibility has been realized in a synthetic system using a peptide amphiphile (PA), which was used in a biomineralization application (Fig. 5).<sup>34</sup> The PA has several functional domains. In short, one of the most important structural characteristics of a PA is a hydrophilic functional peptide domain and a hydrophobic self-assembly domain. The functional peptide domain contains an RGD sequence and a phosphoserine, and the self-assembling domain a fatty acid chain and cysteins for covalent capture. The phosphorylated serine residue interacts strongly with calcium ions and helps direct mineralization of hydroxyapatite. At some specific condition, the combination of hydrophobic,  $\beta$ -sheet, and  $\alpha$ -helical interactions among PA molecules resulted in the formation of birefringent gels, which consisted of a network

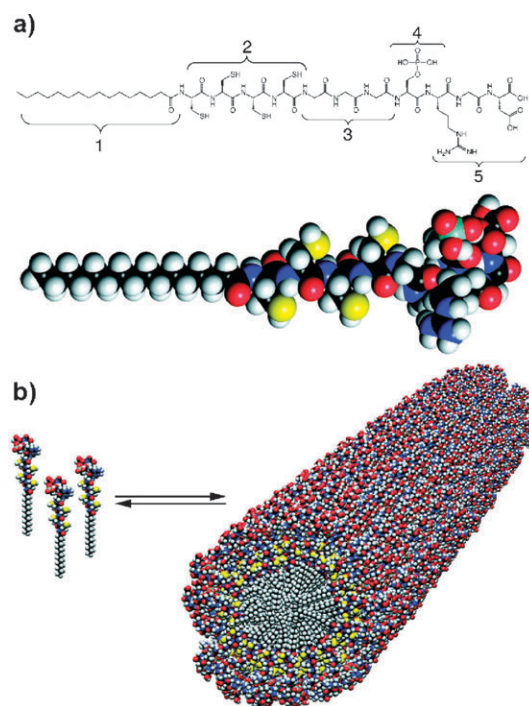


**Fig. 5** (a) Chemical structure of PA. (b) Schematic showing the self-assembly of PA molecules into a cylindrical micelle. Reproduced in part from ref. 34. © 2001 American Association for the Advancement of Science. Used with permission.

of fibers with a diameter of about 8 nm and lengths up to several micrometres. Mineralization experiments show that PA fibers are able to nucleate hydroxyapatite (HA) crystal formation on their surfaces. Importantly, the HA crystal growth was not random, but was co-aligned with the long axes of the fibers.

The usefulness of PA fibers was further exemplified in several different bioapplications. In one study, the pentapeptide epitope (IKVAV), which promotes neurite sprouting and directs neurite growth, was displayed on the surface of PA fibers.<sup>35</sup> These nanofibers bundle to form 3D networks, which provide a 3D scaffold for cell culture. Due to the high surface area, the nanofibers that form around cells in 3D present the epitopes at an artificially high density relative to a natural extracellular matrix. Indeed, neural progenitor cells encapsulated in the network with nanofibers presenting the epitope on their surface differentiated rapidly into neurons. In another study, nanofibers were coated with heparin binding peptides.<sup>19</sup> This process yields nanofibers that display heparin chains to bind and activate angiogenic growth factors for cell signalling. *In vivo*, the nanostructures stimulated extensive new blood vessel formation using nanogram amounts of growth-factor proteins that by themselves did not induce any detectable angiogenesis.

PA fibers could also be used as enzyme mimetics. Given the presence of histidine residues at the catalytic site of several hydrolytic enzymes, a PA fiber decorated with histidines was fabricated as an enzyme mimetic.<sup>36</sup> It was found that the hydrolysis efficiency of DNPA, a model ester compound, benefited from a high density of reactive sites displayed on

the surface of a supramolecular catalytic particle. Notably, a considerably higher hydrolysis rate was observed in the presence of internally ordered supramolecular nanofibers at the catalytic particles, compared to catalysts in solution and in spherical aggregates which should have less internal order.

Morphologies of self-assembled nanostructures are diverse. Spherical micelles, cylindrical micelles, vesicles, and planar membranes are typical examples of self-assembled morphologies in aqueous solution. In addition, there exist nanotubes, toroids, nanosheets, porous membranes, porous vesicles, and helical nanofibers as self-assembled morphologies. Many parameters are responsible for determining nanostructural morphology. Among them, the relative volume fraction between the hydrophilic and the hydrophobic segments has been found to be particularly important for the shape determination.

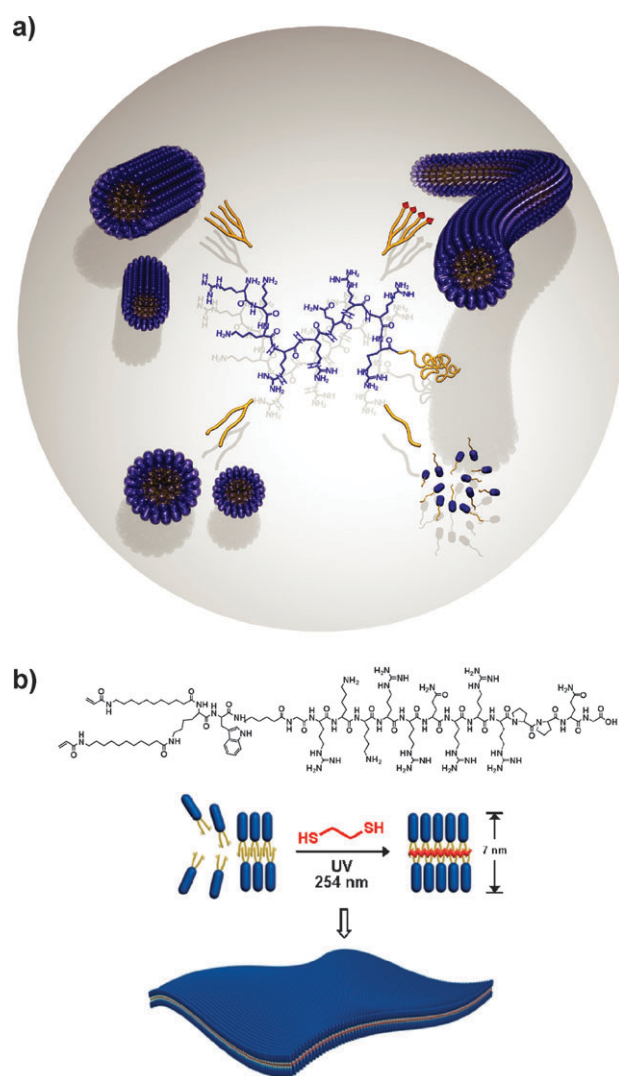


**Fig. 6** (a) Various morphologies of self-assembled nanostructures formed from Tat-CPP/fatty acid dendrimers (TLDs). The fatty acid chain and the linker segment of the TLDs are shown in yellow. (b) Covalent capture of the Tat-CPP-coated nanostructure by thiol-ene photopolymerization. Reproduced in part from ref. 38. © 2008 The Royal Society of Chemistry. Used with permission.

The utilization of the volume fraction concept in the self-assembly of a Tat-CPP-based amphiphilic building block (TLD) has been reported (Fig. 6a).<sup>37</sup> To systematically study the effect of the relative volume fraction of the hydrophobic block in the amphiphilic peptide, the number of fatty acid chains attached to the N-terminus of Tat-CPP was dendritically increased from one to eight. Investigation of the nanostructures revealed that not only control of the shape of peptide-coated nanostructures, but also control of the size and stability is feasible by this molecular manipulation approach. It is notable that the shape of such a nanostructure does not follow the simple function of relative volume fraction. It is likely that the self-assembly behavior of amphiphilic building blocks containing a highly charged hydrophilic segment such as Tat-CPP might not follow the classical volume fraction theory exactly.

The study also stressed the importance of nanostructural stability in cell cytotoxicity. Cytotoxicity experiments suggest that weakly stable nanostructures disintegrate and/or exist as isolated molecules during interaction with the plasma membrane due to their weak association strength, thereby lysing cell membranes in a similar manner to conventional surfactants. In contrast, the cytotoxicity of stable nanostructures was similar to that of unimolecular Tat-CPP; this suggests that the association force of this nanostructure is strong enough to maintain their self-assembled state during cell internalization. As an example of a bioapplication, hydrophobic guest molecules were encapsulated within the interior of the stable nanostructures, and cell delivery was tested. The intracellular delivery experiment revealed that the cell delivery was highly efficient. The cargo molecules were delivered even into the nucleus as well as the cytoplasmic compartment. The compact size of the nanostructures ( $\sim 10 \times 100$  nm, the width and length of a cylindrical micelle) and the multivalent presentation of Tat-CPP are likely to be responsible for this efficient cell delivery activity.

Based on this result, a covalent capture strategy was envisioned to overcome the intrinsic instability of bioactive nanostructures (Fig. 6b).<sup>38</sup> For covalent capture, the building block was designed to incorporate polymerizable acrylamide groups at the distal part of hydrophobic alkyl chains. Once the building blocks aggregated to form self-assembled nanostructures, they were crosslinked together by thiol-ene polymerization reaction. The shape of the nanostructure, 2D sheets, did not change even after the crosslinking reaction. Most importantly, the cytotoxicity experiment showed that the unpolymerized nanostructure was highly toxic, whereas the polymerized nanostructure was nearly nontoxic. This finding demonstrates that covalent capture can become a general means for lowering the cytotoxicity of marginally stable nanostructures.

### 2.3 Mode of self-assembly: interaction between helices

Helical structures are abundant in biological systems. For example, a number of helical structures are found in proteins, which include the  $\alpha$ -helix, polyproline helix, collagen helix,  $3_{10}$ -helix, and  $\pi$ -helix. The polypeptide helices are stabilized by hydrogen bonding and/or steric effects, resulting in them

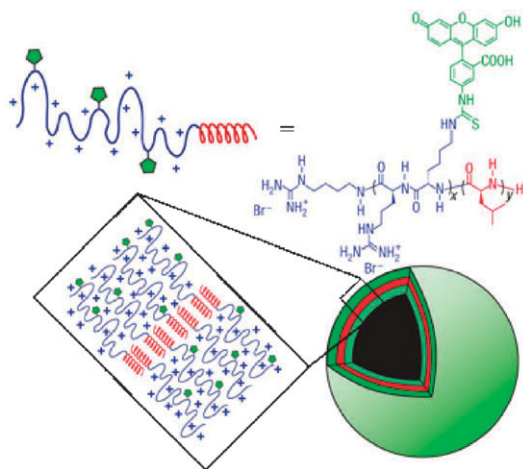


**Fig. 7** Schematic diagram of proposed self-assembly of poly(L-arginine)-*b*-poly(L-leucine). Helical rod, red; coil, blue. Reproduced in part from ref. 41. © 2007 Nature Publishing Group. Used with permission.

having stiff rod-like character. For example, the  $\alpha$ -helix, one of the most common motifs in the secondary structure of proteins, adopts a right-handed helical conformation and is stabilized by hydrogen bonding between amino acids at  $i$  and  $i + 4$  positions. Due to the stiffness of the helical structures, it can have unique self-assembly behavior. Block molecules composed of a hydrophobic helical rod and a hydrophilic coil are one of the examples of rod-coil amphiphiles (rod-coils).<sup>11,20,39</sup> The self-assembly of rod-coils is directed by microphase separation of the two dissimilar blocks similarly to conventional coil-coil amphiphiles (coil-coils). In contrast to coil-coils, rod-coils can form well-ordered structures even at low molecular weights because the anisotropic molecular shape and stiff rod-like conformation of the rod blocks impart orientational organization. The difference in chain rigidity of the stiff rod and the flexible coil block greatly affect the details of molecular packing and thus the nature of thermodynamically stable supramolecular structures. The energetic penalties associated with chain stretching of the coil block and interfacial energy result in the self-assembly of rod-coils into a variety of supramolecular nanostructures depending on the relative volume fraction of the rod segments and temperature.

The self-assembly behavior and bioapplication of peptide rod-coils, such as poly(L-lysine)-*b*-poly(L-leucine), poly(L-glutamic acid)-*b*-poly(L-leucine), and poly(L-arginine)-*b*-poly(L-leucine) diblock polypeptides, have been reported (Fig. 7).<sup>40,41</sup> The driving force underlying the aggregation of the diblock polypeptides was the  $\alpha$ -helical hydrophobic rod formation of the poly(L-leucine) block. Notably, the diblock polypeptides formed vesicular structures at low hydrophobic residue contents (10–40 mol%). Conventional amphiphilic diblock copolymers within this composition range would be expected to form small spherical or cylindrical micelles in aqueous solution, whereas stable vesicles would usually form at higher hydrophobic contents (approximately 30–60 mol%).<sup>42</sup> The copolypeptides should deviate from this trend due to the rigid chain conformation and strong interactions between chains. The formation of micelles with a large degree of interfacial

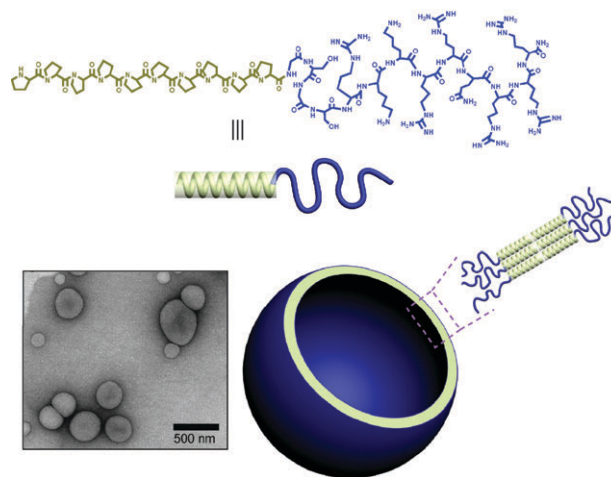


**Fig. 8** Self-assembly of polyproline/Tat-CPP rod-coils. Reproduced in part from ref. 43. © 2008 The Royal Society of Chemistry. Used with permission.

curvature between the hydrophobic and hydrophilic domains is thus disfavored, as the rod-like amphiphiles would rather laterally associate into a flat membrane of relatively low interfacial curvature. The polyarginine-coated vesicles showed potential as intracellular delivery carriers following entrapment of water soluble molecules. The guanidinium residues of arginines, essential residues for the function of CPP, were responsible for the effective intracellular delivery of the vesicles and cargos.

Recently, the self-assembly of peptide rod-coils composed of a polyproline rod and a Tat-CPP coil has been reported (Fig. 8).<sup>43</sup> Among the 20 naturally occurring amino acids, proline is the only one in which the side chain atoms form a pyrrolidine ring with the backbone atoms. As the cyclic structure of proline induces conformational constraints among the atoms in the pyrrolidine ring, the proline-rich sequences tend to form stiff helical rod structures, called a polyproline type II (PPII) helix, in aqueous solution. The hydrophobicity of proline itself as an isolated amino acid is rather small. However, three nonpolar methylene groups are aligned at the outer part of the rod after PPII helix formation. Based on these facts, it was hypothesized that the stiff rod character and the nonpolar nature of the outer surface of the PPII helix might impart microphase separation characteristics to the rod-coil of a PPII rod and a hydrophilic Tat-CPP coil, leading to the anisotropic orientational ordering of the rod and self-assembly. The results showed that the peptide rod-coil did aggregate into a vesicular structure. To assess the potential of the CPP-coated capsule in intracellular delivery of hydrophilic drugs, a water soluble fluorescent dye, rhodamine B, was entrapped within the aqueous space of the capsule. The intracellular delivery experiment performed in a mammalian cell line showed the efficient cell delivery potential of the CPP-coated capsule.

### 3. Carbohydrates as bioactive functional groups

Molecules in biological systems constantly interact with each other for signal communication and specific recognition.

In addition to protein- and nucleic acid-mediated interactions, there are a number of important biological phenomena which depend on carbohydrate-mediated interactions.<sup>44</sup> Carbohydrates generally interact with proteins or other carbohydrates as binding partners. They achieve their specificity by exploring the wide structural diversity of carbohydrates. For example, carbohydrate molecules on the mammalian cell surface are the targets of many pathogenic bacteria and viruses in their initial cell recognition events. Here, multivalent interactions often play crucial roles.<sup>16–18</sup> The pathogens overcome an otherwise weak monovalent carbohydrate–protein interaction ( $K_d = 10^{-3}$ – $10^{-4}$  M<sup>-1</sup>) with multivalent interactions for tight and specific binding, which is then followed by infection of the host cells.

Conventionally, carbohydrate-mediated multivalent interactions have been explored using polymers or dendrimers as scaffolds for carbohydrates attachment.<sup>45</sup> In recent years, self-assembled nanostructures have begun to emerge as multivalent scaffolds for carbohydrate coating.<sup>18</sup> A recent series of studies revealed the clear dependence of carbohydrate-mediated multivalent interactions on nano-object size and shape. By adjusting the relative volume fraction between hydrophilic and hydrophobic segments of rod–coil amphiphiles, it has been possible to control the size and shape of carbohydrate-coated nanostructures, from spheres to vesicles and cylinders.<sup>46,47</sup> The molecular design was implemented by varying either the PEO coil length or the aromatic rod length. As the surfaces of all the nanostructures are covered densely with carbohydrate mannoses, they were shown to act as multivalent ligands in the presence of mannose-binding lectin protein, concanavalin A (Con A). From the increased objects size in TEM images, lectin proteins were found to tightly surround the supramolecular object through multivalent interactions. Such a specific binding event was found exclusively in mannose-decorated nanostructures, as the control experiment with non-specific galactose-decorated objects did not show any specific object–Con A association behavior. Through a hemagglutination inhibition assay with Con A, the influence of nano-architecture on the lectin binding activity was investigated. Hemagglutination assay measures the extent of inhibition of Con A-mediated erythrocyte agglutination. The results showed that, depending on the size and shape of the nanostructures, the inhibitory potency dramatically increased, compared to monomeric carbohydrate. It is worth noting that the inhibition activity varied from object to object (from 800 to 1800 fold). Lessons from these results are that first, molecular self-assembly is well suited for constructing multivalent carbohydrate ligands and second, the biological activity of carbohydrate-decorated supramolecular objects is critically dependent on their size and shape.

Dependence of nanostructural size and shape in supramolecular multivalent interactions was further investigated and corroborated in the carbohydrate–bacterial cell interaction system. For this, triblock rigid–flexible dendritic block molecules consisting of a rigid aromatic segment as a stem segment, carbohydrate (mannose) dendrons as a flexible head, and a hydrophobic alkyl chain were synthesized, and characterized in both the bulk and solution states (Fig. 9).<sup>48</sup> Besides some interesting properties in the bulk state, such

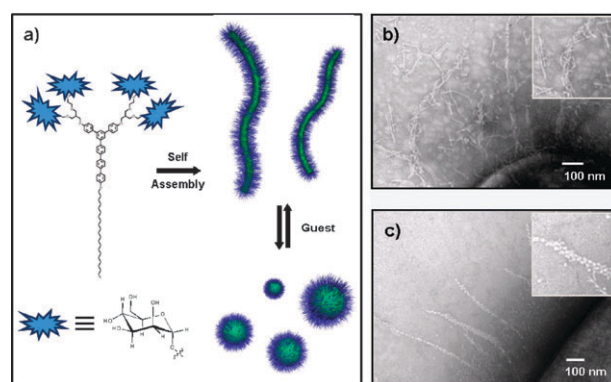


**Fig. 9** (a) Schematic representation of reversible transformation of carbohydrate-coated nanostructures depending on guest encapsulation. TEM images of *E. coli* pili bound with (b) cylindrical and (c) spherical micelles. Reproduced in part from ref. 48. © 2007 American Chemical Society. Used with permission.

building blocks were observed to self-assemble into carbohydrate-coated cylindrical nanostructures with a length of about 200 nm in aqueous solution. Notably, these cylindrical objects were reversibly transformed into spherical objects upon encapsulation (intercalation) of hydrophobic guest molecules. The cylinder to sphere transition was explained as the loosening of rod packing due to the intercalation. To investigate interactions between the mannose-coated nanostructures and the bacterial cells, an *E. coli* strain containing mannose-binding adhesin FimH in its type 1 pili (ORN178)<sup>49</sup> was used. The type 1 pili are filamentous proteinaceous appendages produced by many members of the gram-negative bacteria.<sup>50</sup> Results showed that both nanostructures (cylinder and sphere) could inhibit the motility of bacteria; however, the degree of motility inhibition was significantly dependent on the shape and size of the nanostructures. The inhibition of bacterial motility can be explained by the interference in flagella motion induced by multiple nanostructure binding events.

Based on these results, it can be expected that nanostructures might be able to crosslink and thereby agglutinate bacterial cells if the nanostructures are longer than bacterial cells. *E. coli* cells are typically ~1 μm in length. To show this possibility, building blocks were designed to form a long nanostructure as well as, as a negative control, a short nanostructure (Fig. 10).<sup>51</sup> Both building blocks consist of a carbohydrate mannose, an oligo(ethylene glycol) linker, and a β-sheet assembly peptide. The lengths of the short and the long nanostructures (β-ribbons) were about 200 nm and on the order of a micrometre, respectively. It was shown that β-ribbon length had a marked influence on their interaction with ORN178 bacterial cells. Upon addition of the mannose-coated long β-ribbon to the bacterial suspension, the bacteria lost their motility and agglutinated, whereas the short β-ribbon only inhibited bacterial motility.

The ability of the carbohydrate-coated β-ribbons to inhibit bacterial motility and to agglutinate bacterial cells could be further finely controlled by applying a building block manipulation approach and a co-assembly strategy.<sup>52</sup> First, the length of self-assembled β-ribbon could be controlled by adjusting the length of PEG linker in the building block.

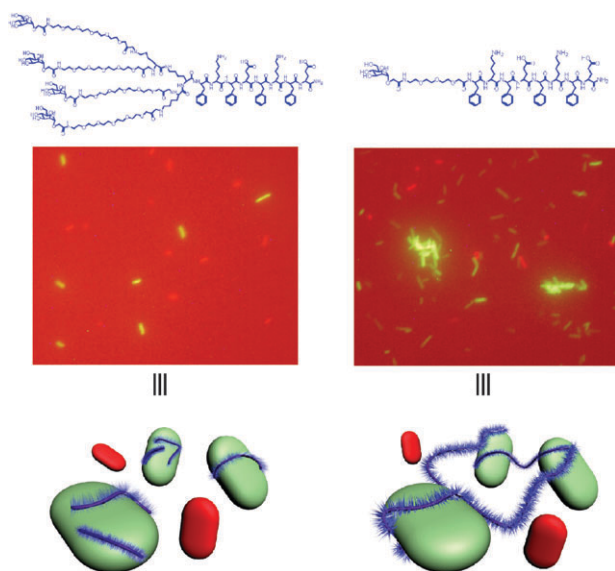


**Fig. 10** Selective motility inhibition and agglutination of bacterial cells by carbohydrate-coated nanostructures. Reproduced in part from ref. 51. © 2007 American Chemical Society. Used with permission.

The results showed that clear positive correlations exist between the length of mannose-coated  $\beta$ -ribbon and the motility inhibition/agglutination. Second, another level of control could be achieved by co-assembling mannose- and glucose-conjugated building blocks together. FimH protein is specific only to mannose residue. In that analogy, the binding affinity of  $\beta$ -ribbon should be decreased as the glucose proportion in the co-assembled  $\beta$ -ribbon increased. The results indicate that bacterial motility and agglutination could be controlled in predictable and tunable ways by changing the composition of the specific and the nonspecific  $\beta$ -ribbon building blocks. Moreover, the carbohydrate-coated  $\beta$ -ribbon could be used to specifically detect bacterial cells with high sensitivity following encapsulation of fluorescent guest molecules. All these results suggested that this type of carbohydrate-coated  $\beta$ -ribbons could be developed as promising agents for specific pathogen capture, clearance, and detection, and that we can finely control the antibacterial activity at will.

Dynamic properties of self-assembled systems can be utilized as a means to optimize the size and shape of multivalent carbohydrate ligands during interaction with multiple receptors.<sup>53</sup> Dendritic rods coupled with carbohydrate ligands (glycodendrimers) were found to self-assemble into noncovalent nanoparticles which could function as polyvalent ligands. A binding assay with decavalent antibody IgM demonstrated the enhancement in protein-carbohydrate binding affinity by the self-assembly and the resulting multivalent carbohydrate presentation. It was suggested that noncovalent multivalent ligands might be rearranged in order to fit into the shape of polyvalent receptors. This is the case when the association force between constituent building blocks is rather weak.

Carbohydrate-coated nanostructures can also be used as multivalent antivirals (Fig. 11).<sup>54</sup> Tetraantennary peptide [glycine<sub>n</sub>-NHCH<sub>2</sub>]<sub>4</sub>C can form submicron-sized, flat, and one-molecule-thick sheets through intermolecular hydrogen bonding of polyglycine II. Attachment of  $\alpha$ -N-acetylneuraminic

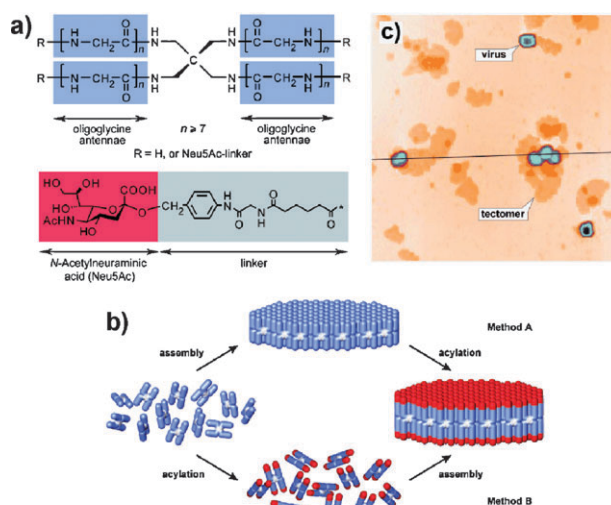


**Fig. 11** (a) Structures of tetraantennary peptide building blocks. (b) Self-assembly of the tetraantennary peptide into nano-sheets. (c) AFM image of influenza viruses captured by the nano-sheets. Reproduced in part from ref. 54. © 2003 Wiley-VCH Verlag GmbH & Co. KGaA. Used with permission.

acid (Neu5Ac $\alpha$ ) receptor for influenza virus to the terminal glycine residue gives rise to water-soluble nanostructures that are able to bind influenza virus multivalently and inhibit adhesion of the virus to cells  $10^3$ -fold more effectively than a monomeric glycoside of Neu5Ac $\alpha$ .

## 4. Conclusions

The field of using self-assembled nanostructures with coated bioactive functions in diverse bioapplications is just beginning to be explored and has shown promising potential. The size of nanostructures is significantly bigger than most small molecules. This unique property can offer novel and unexplored opportunities in developing self-assembled nanostructures as useful biomaterials. In order for this field of research to advance further, ongoing research efforts are necessary in several aspects. First, self-assembled nanostructures should be under control. With the advent of supramolecular science, knowledge of how to control the nanostructural properties such as shape, size, and stability is accumulating. It is becoming evident that the nanostructural properties have a significant influence on the biological activity. Therefore, the physical properties of bioactive nanostructures should be able to be controlled at our discretion for successful bioapplications. Second, nanostructures should be suitably functionalized. The realm of biology is immensely complex and new discoveries are constantly being made by biologists. With this vast potential available, judicious decisions on the types of bioapplications that are going to be pursued should be made in conjunction with nanostructural property controls for a meaningful and useful outcome.

## Acknowledgements

We gratefully acknowledge the National Creative Research Program of the Ministry of Education, Science and Technology.

## References

- 1 J.-M. Lehn, *Proc. Natl. Acad. Sci. U. S. A.*, 2002, **99**, 4763.
- 2 H. Otsuka, *Adv. Drug Delivery Rev.*, 2003, **55**, 403.
- 3 C. Allen, D. Maysinger and A. Eisenberg, *Colloids Surf., B*, 1999, **16**, 3.
- 4 A. G. Barrientos, J. M. de la Fuente, T. C. Rojas, A. Fernández and S. Penadés, *Chem.-Eur. J.*, 2003, **9**, 1909.
- 5 X. Chen, U. C. Tam, J. L. Czapinski, G. S. Lee, D. Rabuka, A. Zettl and C. R. Bertozzi, *J. Am. Chem. Soc.*, 2006, **128**, 6292.
- 6 N. L. Rosi and C. A. Mirkin, *Chem. Rev.*, 2005, **105**, 1547.
- 7 D. W. Pack, A. S. Hoffman, S. Pun and P. S. Stayton, *Nat. Rev. Drug Discovery*, 2005, **4**, 581.
- 8 Y.-b. Lim, C.-h. Kim, K. Kim, S. W. Kim and J.-s. Park, *J. Am. Chem. Soc.*, 2000, **122**, 6524.
- 9 Y. He, T. Ye, M. Su, C. Zhang, A. E. Ribbe, W. Jiang and C. Mao, *Nature*, 2008, **452**, 198.
- 10 W. H. Binder, *Angew. Chem., Int. Ed.*, 2005, **44**, 5172.
- 11 M. Lee, B.-K. Cho and W.-C. Zin, *Chem. Rev.*, 2001, **101**, 3869.
- 12 V. Percec, A. E. Dulcey, V. S. K. Balagurusamy, Y. Miura, J. Smidrkal, M. Peterca, S. Nummelin, U. Edlund, S. D. Hudson, P. A. Heiney, H. Duan, S. N. Magonov and S. A. Vinogradov, *Nature*, 2004, **430**, 764.
- 13 M. A. Alam, Y.-S. Kim, S. Ogawa, A. Tsuda, N. Ishii and T. Aida, *Angew. Chem., Int. Ed.*, 2008, **47**, 2070.
- 14 J. A. A. W. Elemans, A. E. Rowan and R. J. M. Nolte, *J. Mater. Chem.*, 2003, **13**, 2661.
- 15 V. Daggett and A. R. Fersht, *Trends Biochem. Sci.*, 2003, **28**, 18.
- 16 M. Mammen, S. K. Choi and G. M. Whitesides, *Angew. Chem., Int. Ed.*, 1998, **37**, 2755.
- 17 L. L. Kiessling, J. E. Gestwicki and L. E. Strong, *Angew. Chem., Int. Ed.*, 2006, **45**, 2348.
- 18 Y.-b. Lim and M. Lee, *Org. Biomol. Chem.*, 2007, **5**, 401.
- 19 K. Rajangam, H. A. Behanna, M. J. Hui, X. Han, J. F. Hulvat, J. W. Lomasney and S. I. Stupp, *Nano Lett.*, 2006, **6**, 2086.
- 20 Y.-b. Lim, K.-S. Moon and M. Lee, *J. Mater. Chem.*, 2008, **18**, 2909.
- 21 I. Cherny and E. Gazit, *Angew. Chem., Int. Ed.*, 2008, **47**, 4062.
- 22 Y.-b. Lim and M. Lee, *J. Mater. Chem.*, 2008, **18**, 723.
- 23 C. W. G. Fishwick, A. J. Beevers, L. M. Carrick, C. D. Whitehouse, A. Aggeli and N. Boden, *Nano Lett.*, 2003, **3**, 1475.
- 24 T. S. Burkoth, T. L. S. Benzinger, D. N. M. Jones, K. Hallenga, S. C. Meredith and D. G. Lynn, *J. Am. Chem. Soc.*, 1998, **120**, 7655.
- 25 Y.-b. Lim, E. Lee and M. Lee, *Angew. Chem., Int. Ed.*, 2007, **46**, 3475.
- 26 S. Futaki, *Adv. Drug Delivery Rev.*, 2005, **57**, 547.
- 27 M. L. Janssen, W. J. Oyen, I. Dijkgraaf, L. F. Massuger, C. Frielink, D. S. Edwards, M. Rajopadhye, H. Boonstra, F. H. Corstens and O. C. Boerman, *Cancer Res.*, 2002, **62**, 6146.
- 28 Y.-b. Lim, O.-J. Kwon, E. Lee, P.-H. Kim, C.-O. Yun and M. Lee, *Org. Biomol. Chem.*, 2008, **6**, 1944.
- 29 Y.-b. Lim, E. Lee, Y.-R. Yoon, M. S. Lee and M. Lee, *Angew. Chem., Int. Ed.*, 2008, **47**, 4525.
- 30 A. J. Baldwin, R. Bader, J. Christodoulou, C. E. MacPhee, C. M. Dobson and P. D. Barker, *J. Am. Chem. Soc.*, 2006, **128**, 2162.
- 31 U. Baxa, V. Speransky, A. C. Steven and R. B. Wickner, *Proc. Natl. Acad. Sci. U. S. A.*, 2002, **99**, 5253.
- 32 H. Kodama, S. Matsumura, T. Yamashita and H. Mihara, *Chem. Commun.*, 2004, 2876.
- 33 J. S. Martinez, G. P. Zhang, P. D. Holt, H.-T. Jung, C. J. Carrano, M. G. Haygood and A. Butler, *Science*, 2000, **287**, 1245.
- 34 J. D. Hartgerink, E. Beniash and S. I. Stupp, *Science*, 2001, **294**, 1684.
- 35 G. A. Silva, C. Czeisler, K. L. Niece, E. Beniash, D. A. Harrington, J. A. Kessler and S. I. Stupp, *Science*, 2004, **303**, 1352.
- 36 M. O. Guler and S. I. Stupp, *J. Am. Chem. Soc.*, 2007, **129**, 12082.
- 37 Y.-b. Lim, E. Lee and M. Lee, *Angew. Chem., Int. Ed.*, 2007, **46**, 9011.
- 38 K.-S. Moon, E. Lee, Y.-b. Lim and M. Lee, *Chem. Commun.*, 2008, 4001.
- 39 J.-H. Ryu, D.-J. Hong and M. Lee, *Chem. Commun.*, 2008, 1043.
- 40 E. G. Bellomo, M. D. Wyrsta, L. Pakstis, D. J. Pochan and T. J. Deming, *Nat. Mater.*, 2004, **3**, 244.
- 41 E. P. Holowka, V. Z. Sun, D. T. Kamei and T. J. Deming, *Nat. Mater.*, 2007, **6**, 52.
- 42 B. M. Discher, D. A. Hammer, F. S. Bates and D. E. Discher, *Curr. Opin. Colloid Interface Sci.*, 2000, **5**, 125.
- 43 Y.-R. Yoon, Y.-b. Lim, E. Lee and M. Lee, *Chem. Commun.*, 2008, 1892.
- 44 C. R. Bertozzi and L. L. Kiessling, *Science*, 2001, **291**, 2357.
- 45 S.-K. Choi, *Synthetic multivalent molecules*, John Wiley & Sons Inc., New Jersey, 2004.
- 46 B.-S. Kim, W.-Y. Yang, J.-H. Ryu, Y.-S. Yoo and M. Lee, *Chem. Commun.*, 2005, 2035.
- 47 B.-S. Kim, D.-J. Hong, J. Bae and M. Lee, *J. Am. Chem. Soc.*, 2005, **127**, 16333.
- 48 J.-H. Ryu, E. Lee, Y.-b. Lim and M. Lee, *J. Am. Chem. Soc.*, 2007, **129**, 4808.
- 49 S. L. Harris, P. A. Spears, E. A. Havell, T. S. Hamrick, J. R. Horton and P. E. Orndorff, *J. Bacteriol.*, 2001, **183**, 4099.
- 50 C. C. Lin, Y. C. Yeh, C. Y. Yang, C. L. Chen, G. F. Chen, C. C. Chen and Y. C. Wu, *J. Am. Chem. Soc.*, 2002, **124**, 3508.
- 51 Y.-b. Lim, S. Park, E. Lee, H. Jeong, J.-H. Ryu, M. S. Lee and M. Lee, *Biomacromolecules*, 2007, **8**, 1404.
- 52 Y.-b. Lim, S. Park, E. Lee, J.-H. Ryu, Y.-R. Yoon, T.-H. Kim and M. Lee, *Chem.-Asian J.*, 2007, **2**, 1363.
- 53 G. Thoma, A. G. Katopodis, N. Voelcker, R. O. Duthaler and M. B. Streiff, *Angew. Chem., Int. Ed.*, 2002, **41**, 3195.
- 54 A. B. Tuzikov, A. A. Chinarev, A. S. Gambaryan, V. A. Oleinikov, D. V. Klinov, N. B. Matsko, V. A. Kadykov, M. A. Ermishov, I. V. Demin, V. V. Demin, P. D. Rye and N. V. Bovin, *ChemBioChem*, 2003, **4**, 147.